MOLECULAR AND CELLULAR BIOLOGY, Nov. 2004, p. 9383–9389 Vol. 24, No. 21
0270-7306/04/$08.00+0 DOI: 10.1128/MCB.24.21.9383–9389.2004

ALK7, a Receptor for Nodal, Is Dispensable for Embryogenesis and Left-Right Patterning in the Mouse

Henrik Jörnvall, Eva Reissmann,† Olov Andersson,† Mehrnaz Mehrkash, and Carlos F. Ibáñez*

Division of Molecular Neurobiology, Department of Neuroscience, Karolinska Institute, Stockholm, Sweden

Received 2 March 2004/Returned for modification 17 May 2004/Accepted 3 August 2004

Mesendoderm formation and left-right patterning during vertebrate development depend upon selected members of the transforming growth factor β superfamily, particularly Nodal and Nodal-related ligands. Two type I serine/threonine kinase receptors have been identified for Nodal, ALK4 and ALK7. Mouse embryos lacking ALK4 fail to produce mesendoderm and die shortly after gastrulation, resembling the phenotype of Nodal knockout mice. Whether ALK4 contributes to left-right patterning is still unknown. Here we report the generation and initial characterization of mice lacking ALK7. Homozygous mutant mice were born at the expected frequency and remained viable and fertile. Viability at weaning was not different from that of the wild type in *ALK7*$^{-/-}$; *Nodal*$^{+/-}$ and *ALK7*$^{-/-}$; *ALK4*$^{+/-}$ compound mutants. *ALK7* and *ALK4* were highly expressed in interdigital regions of the developing limb bud. However, *ALK7* mutant mice displayed no skeletal abnormalities or limb malformations. None of the left-right patterning abnormalities and organogenesis defects identified in mice carrying mutations in *Nodal* or in genes encoding ActRIIA and ActRIIB coreceptors, including heart malformations, pulmonary isomerism, right-sided gut, and spleen hypoplasia, were observed in mice lacking ALK7. Finally, the histological organization of the cerebellum, cortex, and hippocampus, all sites of significant ALK7 expression in the rodent brain, appeared normal in *ALK7* mutant mice. We conclude that ALK7 is not an essential mediator of Nodal signaling during mesendoderm formation and left-right patterning in the mouse but may instead mediate other activities of Nodal and related ligands in the development or function of particular tissues and organs.

The formation of the mesodermal and endodermal germ layers is one of the earliest induction events during vertebrate embryogenesis. Genetic experiments with mouse and zebra fish have indicated that Nodal and related factors are required for mesendoderm formation (18). Mouse embryos lacking Nodal, the only family member identified in mammals, die shortly after gastrulation without forming a node, an organizing center similar to the dorsal lip of frog embryos that is responsible for the formation of axial mesoderm (5, 25). Although genetic experiments have indicated that the transforming growth factor β family member Activin is not required for mesendoderm formation, its ability to induce mesodermal markers upon overexpression in the early embryo has indicated that this protein may activate some component of the Nodal signaling pathway, including putative Nodal receptors. In agreement with this, the Activin type I receptor ALK4 has been shown to form a receptor complex for Nodal together with Activin type II receptors ActRIIA and ActRIIB and the extracellular protein Cripto, a member of the epidermal growth factor (EGF)–Cripto-FRL1-cryptic (CFC) family of glycosyl phosphatidylinositol-anchored proteins (16, 24). This notion is supported by loss- and gain-of-function studies indicating a role for Activin receptors and Cripto in Nodal signaling. Thus, a null mutation of *Cripto* abolishes mesendoderm formation (6). In addition, mice lacking ActRIIB have defects in left-right axis formation, and compound *ActRIIA* and *ActRIIB* mutants recapitulate all of the typical deficits of Nodal loss of function (2, 14, 19). Gain-of-function experiments with a constitutively activated form of ALK4 have demonstrated the ability of this receptor to induce mesendoderm and formation of a secondary axis in whole embryos (1, 3), and the phenotype of a null mutation in the mouse *ALK4* gene resembles that of the Nodal knockout (9).

In addition to ALK4, the type I receptor ALK7 has also been found to mediate signaling by Nodal and related proteins (16). Unlike ALK4, however, ALK7 was capable of transmitting Nodal signals even in the absence of Cripto, albeit less efficiently (16), suggesting that ALK7 may have a higher affinity for Nodal ligands than ALK4. *ALK7* mRNA has been localized to the ectodermal and organizer regions of *Xenopus* gastrula embryos, and low but detectable levels have also been found in the early mouse embryo (16). ALK7 is expressed predominantly in distinct subpopulations of cells in the rodent central nervous system during postnatal development, primarily cerebellum, hippocampus, cortex, and brain stem nuclei (12, 17, 20). *ALK7* mRNA expression has also been detected to various degrees in a few peripheral organs and tissues, such as gut, kidney, ovary, pancreas, brown fat, and hair follicles (12, 17, 20). ALK7 is most similar in its serine/threonine kinase domain to ALK4 and ALK5 but is very divergent from all other ALK receptors in its extracellular domain (17). ALK7 signaling, as evaluated with a constitutively active mutant receptor, resembles that of Activin and transforming growth factor β in that it activates Smad2 and Smad3 but not Smad1 (10, 21).

Here we report the generation and initial characterization of mutant mice lacking ALK7. In this study, we have focused our analysis on possible phenotypes resembling Nodal loss of function, as well as possible defects in brain structures where *ALK7* mRNA expression is concentrated.

* Corresponding author. Mailing address: Department of Neuroscience, Karolinska Institute, Retzius väg 8, S-17177 Stockholm, Sweden. Phone: 46 8 5248 7660. Fax: 46 8 33 95 48. E-mail: carlos.ibanez@neuro.ki.se.

† E.R. and O.A. contributed equally to this work.

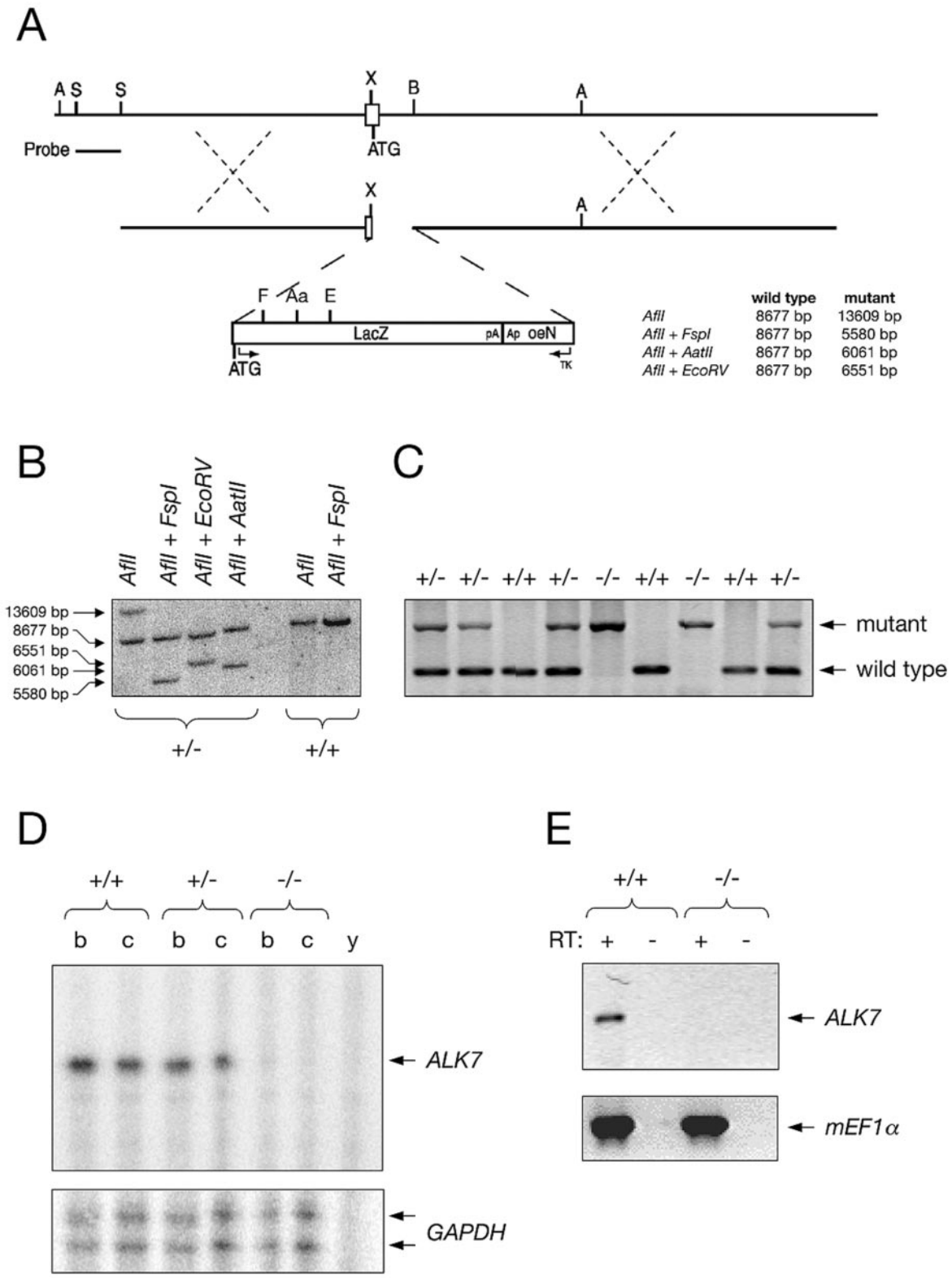

FIG. 1. Generation of *ALK7* mutant mice by homologous recombination in ES cells. (A) Diagrams of the targeted locus and construct used for the generation of *ALK7* null mice. The external probe used for Southern blotting analysis is indicated. See Materials and Methods for details. A, AflII; Aa, AatII; E, EcoRV; F, FspI; S, StuI, X, XmaI; B, BspEI. Fragment sizes expected after the indicated restriction enzyme cleavages are noted. (B) Southern blotting analysis of two ES cell clones with the indicated restriction enzymes. One of the clones (+/−) carries a targeted allele. (C) PCR analysis of tail DNA from the progeny of an intercross between two heterozygous mutant mice. Bands corresponding to the mutant and wild-type alleles are indicated. (D) RNase protection assay of *ALK7* mRNA expression in adult brain (b) and cerebellum (c) of wild-type (+/+), heterozygous (+/−), and homozygous (−/−) *ALK7* mutant mice. y, yeast tRNA control. The signal obtained with the glyceraldehyde-3-phosphate dehydrogenase (GAPDH) probe added to the reaction mixture (lower panel) was used as loading control. (E) RT-PCR analysis of *ALK7* mRNA expression in E8.5 wild-type (+/+) and *ALK7* mutant (−/−) embryos. RT, reverse transcriptase; c, control without input cDNA. Expression of the mouse elongation factor 1 alpha (mEF1α) (lower panel) was used as loading control.

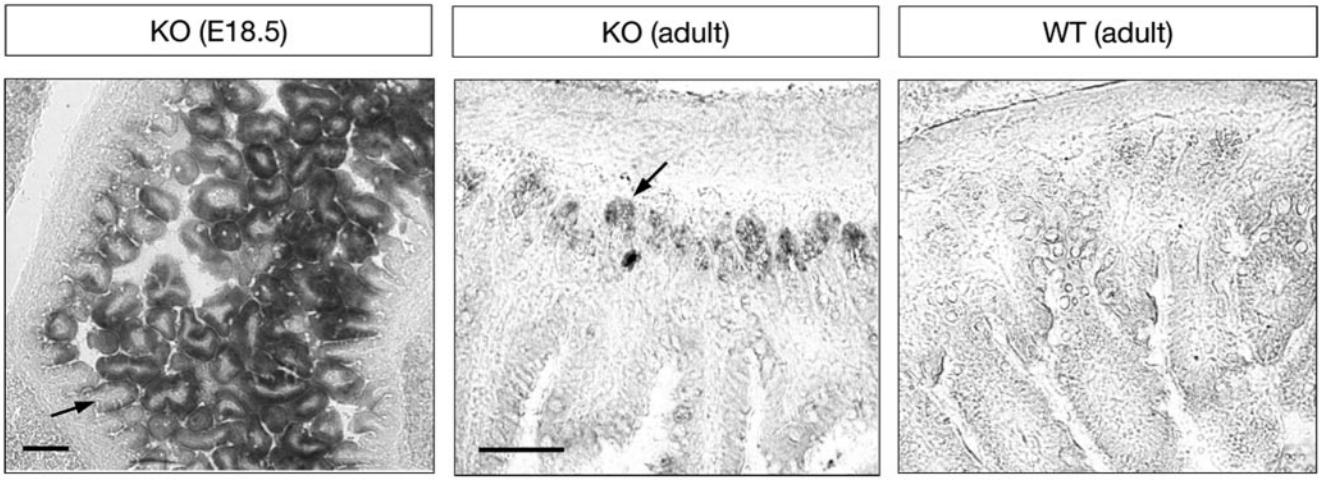

FIG. 2. Expression of *lacZ* from the *ALK7* locus recapitulates *ALK7* expression in embryonic and adult gut. Shown are sections through E18.5 mutant gut (left) and adult mutant (knockout [KO]) and wild-type (WT) gut processed for β-galactosidase histochemistry. Arrows indicate *lacZ*-expressing cells in the outer layer of the tips of the villi lining the internal wall of the intestine (E18.5) and in the crypt, a proliferative region located between the smooth muscle layer and the intestine mucosa (adult). No *lacZ* staining was observed in the guts of wild-type animals. Bars, 100 (left panel) and 50 μm (right panel).

MATERIALS AND METHODS

Targeting of the *ALK7* locus. A murine 129/Sv lambda FIX II genomic phage library (Stratagene) was screened with a 110-bp probe from the ATG domain of rat ALK7 (corresponding to nucleotides −17 to +93). A 14.1-kb clone containing 220 bp with high similarity to the cDNA sequence of the rat *ALK7* gene was obtained. A targeting vector was constructed by introducing the bacterial *lacZ* gene reporter in frame with the *ALK7* start codon. A neomycin cassette was inserted in the reverse orientation after the *lacZ* gene. The targeting construct contained 11,177 bp of homology with the endogenous *ALK7* gene, 4,132 bp at the 5′ end and 7,045 bp at the 3′ end (Fig. 1A). The targeting construct was excised with NotI and SalI prior to electroporation into E14 embryonic stem (ES) cells. After neomycin selection, ES cell colonies were screened for homologous recombination events by Southern blotting with a 795-bp external probe (Fig. 1B). Nine positive clones were obtained, of which six were injected into C57BL/6 blastocysts and implanted into the uteruses of pseudopregnant females. Three independent ES cell clones gave germ line transmission of the mutation, and a total of 15 chimeric mice were obtained. Chimeric males corresponding to two different ES cell clones were crossed to either Sv129 or C57BL/6 females. No phenotypic differences were found between mutant animals derived from either ES cell clone. Of note is that earlier attempts to target the kinase and GS domains of *ALK7* failed to yield homologous recombination events after screening of more than 2,200 ES cell colonies.

Genotyping was done by PCR with tail DNA and the following oligonucleotide primers: ALK7wt_sense, TGGGGGACGAAATCATCAAG; ALK7wt_antisense, GCGCACCTGCACCCCTCCAA; ALK7mut_sense, CGCCCCGGGAACTTCAA AGC; and ALK7mut_antisense, TAACAACCCGTCGGATTCTC. Fifteen of the 51 agouti chimera offspring that were obtained could be genotyped as heterozygous for the *ALK7* mutation. Genomic DNA from ES cells and mouse tails was prepared by treatment with lysis buffer (5 mM EDTA, 0.2% [wt/vol] sodium dodecyl sulfate [SDS], 200 mM NaCl, 100 mM Tris-HCl [pH 8.5]; 100 μg of proteinase K per ml), followed by isopropanol precipitation. For Southern blotting, the genomic DNA was cleaved and separated by electrophoresis on a 0.6% agarose gel. The gel was then blotted onto Hybond N+ nylon membranes (Amersham) by overnight alkali transfer according to the manufacturer's instructions. Hybridization was performed in Church buffer (7% [wt/vol] SDS, 1% [wt/vol] bovine serum albumin,10 mM EDTA, 0.5 M phosphate buffer [pH 7.4]) at 65°C with extended hybridization times (at least 1 day of prehybridization and 2 days of hybridization). After hybridization, the membranes were washed in 0.2% (wt/vol) SDS–0.2× SSC (1× SSC is 0.15 M NaCl plus 0.015 M sodium citrate) at 65°C until they were clean. Bands were visualized and quantified by using a STORM840 PhosphorImager and ImageQuant software (Molecular Dynamics).

RNase protection assay and RT-PCR. A 324-bp HindIII/BmrI fragment from a mouse *ALK7* expressed sequence tag (mouse 1196242 vu65a06.r1 pT7T3D-Pac; American Type Culture Collection) corresponding to residues 277 to 381 from the kinase domain was subcloned into pBS, linearized with HindIII, and transcribed with T3 RNA polymerase to generate antisense RNA probes for RNase protection assay. [α-^{32}P]CTP-labeled probes were hybridized with 10 μg of total RNA according to the instructions of the manufacturer (Ambion Inc.). Protected bands were visualized and quantified by using a STORM840 PhosphorImager and ImageQuant software (Molecular Dynamics).

Total RNA extraction was done with an RNeasy kit (Qiagen), followed by DNase I treatment (Invitrogen) and cDNA synthesis (ProStar first-strand reverse transcription-PCR [RT-PCR] kit; Stratagene). RT-PCR for ALK7 was done by using primer sequences located in different exons (ALK7 transmembrane, ACC GCCAGTGCACATACA; ALK7 kinase, TCGTGCTTCACAGCCA), generating a 623-bp fragment from the intracellular domain of the receptor.

Whole-mount in situ hybridization, skeletal preparations, and immunohisto-

TABLE 1. Normal frequency of *ALK7* knockout mice at weaning[a]

Genotype	No. of animals obtained	Frequency (%)	
		Observed	Expected
ALK7$^{+/+}$	85	27.7	25
ALK7$^{+/-}$	144	50.8	50
ALK7$^{-/-}$	77	21.5	25
Total	306	100	100

[a] The fit to Mendelian expectation was tested with a chi-square test: $\chi^2 = 1.48$, degrees of freedom = 2, $P > 0.2$.

TABLE 2. Normal frequency of compound *ALK7*$^{-/-}$; *Nodal*$^{+/-}$ mutant mice at weaning[a]

Genotype	No. of animals obtained	Frequency (%)	
		Observed	Expected
ALK7$^{+/-}$ *Nodal*$^{+/+}$	25	32	25
ALK7$^{+/-}$ *Nodal*$^{+/-}$	12	16	25
ALK7$^{-/-}$ *Nodal*$^{+/+}$	22	28	25
ALK7$^{-/-}$ *Nodal*$^{+/-}$	19	24	25
Total	78	100	100

[a] The fit to Mendelian expectation was tested with a chi-square test: $\chi^2 = 1.24$, degrees of freedom = 3, $P > 0.2$.

TABLE 3. Normal frequency of compound *ALK7*$^{-/-}$; *ALK4*$^{+/-}$ mutant mice at weaning[a]

Genotype	No. of animals obtained	Frequency (%)	
		Observed	Expected
ALK7$^{+/-}$; *ALK4*$^{+/+}$	26	28	25
ALK7$^{+/-}$; *ALK4*$^{+/-}$	19	20	25
ALK7$^{-/-}$; *ALK4*$^{+/+}$	25	27	25
ALK7$^{-/-}$; *ALK4*$^{+/-}$	23	25	25
Total	93	100	100

[a] The fit to Mendelian expectation was tested with a chi-square test: $\chi^2 = 4.77$, degrees of freedom = 3, $0.2 > P > 0.1$.

chemistry. Whole-mount in situ hybridization was performed according to previously published procedures (22), but with proteinase K digestion omitted. The *ALK7* probe was synthesized by using 563 bp of the mouse *ALK7* gene amplified by PCR with primers TTCAAACTTCACCTGCCAAACG and CAGAGGCAG TAGCATCGTAG, cloned into pCRII, linearized with XbaI, and transcribed with SP6 RNA polymerase. The *ALK4* probe has been described previously (9).

Ten-micrometer sections from fresh frozen brain tissue were prepared in a cryostat, mounted on Superfrost slides, and fixed in 4% paraformaldehyde prior to immunostaining. Primary antibodies (Calbindin [Chemicon] and Calretinin [Swant]) were applied overnight at 4°C at a 1:2,000 dilution in phosphate-buffered saline containing 10% goat serum, 0.1% Triton X-100, and 1% bovine serum albumin. Secondary biotin-conjugated anti-rabbit antibody (Vector Labs) was used at a 1:100 dilution in the same buffer for 2 h at room temperature, followed by the peroxidase substrate reaction with the Nove Red kit (Vector Labs). For hematoxylin and eosin stainings, the tissue was processed as described above, followed by staining with hematoxylin (Merck) and 1% eosin Y disodium salt (Sigma) according to standard protocols. Sections were embedded in Permount (Histolab). For radioactive in situ hybridization, sections were processed as described previously (8), using a 50-mer oligonucleotide probe derived from the ectodomain of mouse *ALK7*. *lacZ* expression was detected by β-galactosidase histochemistry in sections fixed in glutaraldehyde according to standard procedures. Tissue sections were examined in an Axioskop microscope (Zeiss) with Openlab image analysis software.

Skeletons from newborn mice were stained with Alcian Blue and Alizarin Red according to standard protocols, with the exception that Alcian Blue and Alizarin Red were added at the same time and incubated overnight.

RESULTS

Generation of *ALK7* mutant mice by homologous recombination in ES cells. A null mutation was introduced in the mouse *ALK7* locus (Acvr1c) by homologous recombination in ES cells by standard techniques. The targeting construct contained over 11 kb of sequence homologous to the endogenous gene and was designed to introduce the *lacZ* reporter gene in frame with the ATG start codon of the *ALK7* locus (Fig. 1A). The mutation resulted in the deletion of 75 bp after the ATG start codon in the 3′ end of the first exon and of 664 bp from the 5′ end of the first intron. The correct targeting event was confirmed by restriction analysis and Southern blotting of genomic DNA from electroporated ES cell clones (Fig. 1B). Three independent ES cell clones gave germ line transmission of the mutation, which was confirmed by PCR analysis of tail DNA (Fig. 1C). Homozygous mutant mice were generated from two of these ES cell clones; no phenotypic differences were observed between mutant animals derived from either clone. No *ALK7* mRNA could be detected in homozygous mutant mice by RNase protection assay (Fig. 1D) or RT-PCR (Fig. 1E), and ALK7 immunoreactivity was absent in pancreas from the mutants (not shown), confirming that we had generated a null mutation. In homozygous mutant mice, expression of the *lacZ* reporter gene could be detected in several organs and tissues that have previously been shown to express *ALK7*

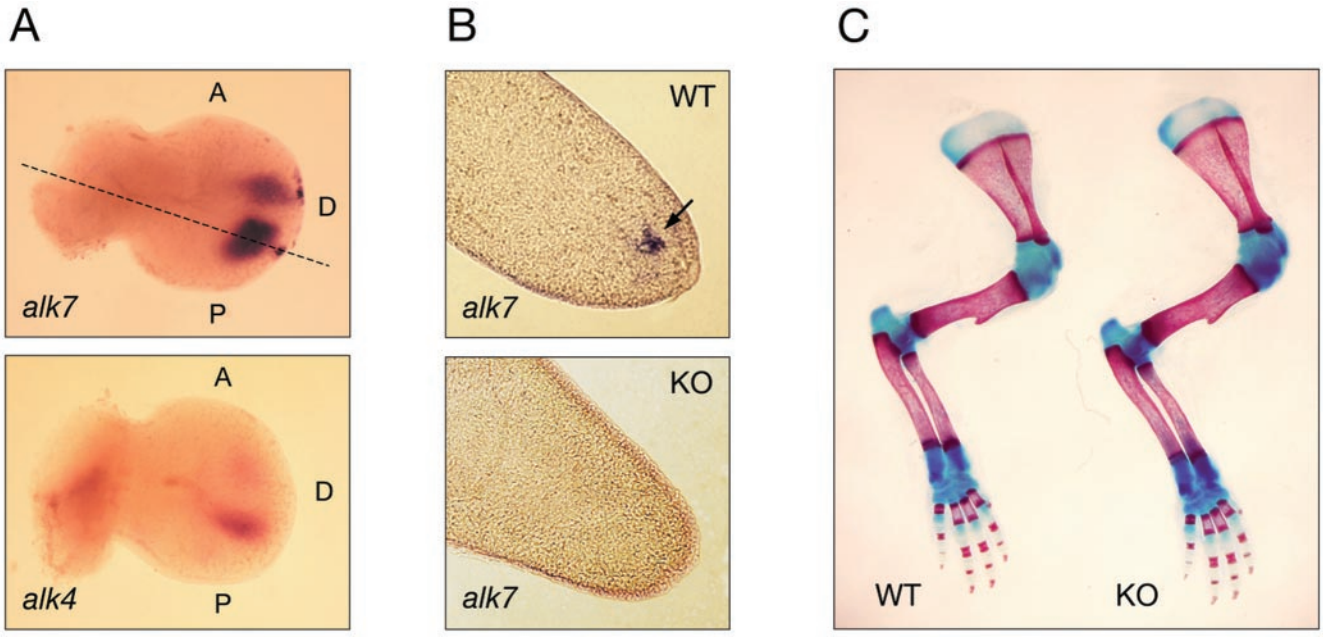

FIG. 3. Overlapping expression of *ALK7* and *ALK4* in interdigital regions and lack of skeletal defects in limbs of *ALK7* mutant mice. (A) Expression of *ALK7* and *ALK4* mRNAs in interdigital regions of limb buds from E12 mouse embryos analyzed by whole-mount in situ hybridization. A, anterior; D, dorsal; P, posterior. (B) Longitudinal sections through the tips of wild-type (WT) and knockout (KO) E12 limb buds (plane indicated by dashed line in panel A) hybridized for *ALK7* mRNA. Note lack of *ALK7* mRNA signal in mutant limb bud. (C) Alcian Blue and Alizarin Red staining of skeletal structures (bone in red and cartilage in blue) from forelimbs of newborn wild-type and *ALK7* mutant (KO) mice.

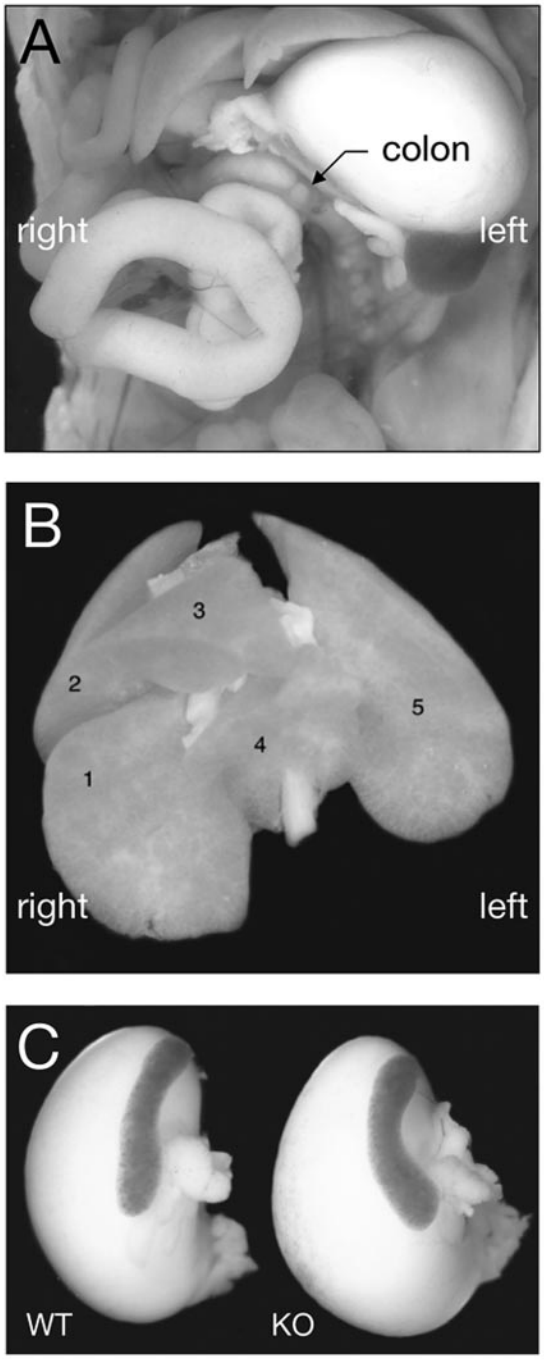

FIG. 4. No left-right patterning defects in mice lacking ALK7. (A) Normal left-sided gut looping in newborn *ALK7* mutant mice. The colon is indicated. (B) Normal lung lobation in newborn *ALK7* mutant mice. Lung lobes are numbered as follows: 1, caudal lung lobe; 2, cranial lung lobe; 3, medial lung lobe; 4, accessory lung lobe; 5, left lung lobe. In right pulmonary isomerism, lobes 1, 2, 3, and 4 are duplicated on the left side. (C) Normal spleen size in newborn *ALK7* mutant mice (knockout [KO]).

mRNA, including gut, kidney, pancreas, and hair follicles. In the gut, strong *lacZ* expression could be detected at embryonic day 18.5 (E18.5) in the outer cell layer of the tips of the villi lining the internal wall of the intestine (Fig. 2A). In the adult gut, *lacZ* staining was confined to the crypt, a proliferative region sandwiched between the smooth muscle layer and the intestine mucosa (Fig. 2B). No *lacZ* staining was observed in the guts of wild-type animals (Fig. 2C), and no gross histological abnormalities could be observed in the guts of *ALK7* mutant mice compared to the wild type. In addition, glycemia and insulinemia in fasted young adult mutant mice were not significantly different from those in the wild type (data not shown). Intriguingly, no *lacZ* staining could be detected in the brains of homozygous mutant mice at any stage of development (not shown). Further RNase protection assay and RT-PCR analyses demonstrated a complete absence of *lacZ* mRNA expression in the brains of homozygous mutant mice (not shown), indicating that the mutation had inactivated the *ALK7* locus in this tissue. Although the reason for the discrepancy between brain and other tissues is unknown, it is possible that the 739-bp segment deleted from the first exon and intron of the *ALK7* gene contains regulatory sequences that are essential for the expression of this gene in brain.

***ALK7* mutant mice are viable and fertile.** $ALK7^{-/-}$ mice developed to normal size and weight on a Chaw diet and were fertile in both inbred Sv129 and mixed Sv129 × C57BL/6 backgrounds. All data reported here are from the 129 inbred line unless otherwise indicated. Animals homozygous for the *ALK7* mutation were observed at the expected frequency in the progeny of heterozygous intercrosses (Table 1), indicating that ALK7 function is dispensable for embryogenesis in the mouse, at least in the absence of additional mutations. We investigated possible genetic interactions between *ALK7*, *Nodal*, and *ALK4* in mouse embryogenesis and viability by crossing homozygous *ALK7* mutant mice with heterozygous *Nodal* and *ALK4* mutants. Although both homozygous *Nodal* and *ALK4* mutants die at early stages of embryonic development, heterozygous animals are normal (4, 9). However, both $ALK7^{-/-}$; $Nodal^{+/-}$ and $ALK7^{-/-}$; $ALK4^{+/-}$ compound mutants were observed at the expected frequencies at weaning (Tables 2 and 3).

Overlapping expression of *ALK7* and *ALK4* in the interdigital regions of developing limb bud. Whole-mount in situ hybridization of E12 mouse embryos revealed distinct expression of *ALK7* mRNA in interdigital regions in developing limb buds, in a pattern that overlapped with that of *ALK4* mRNA (Fig. 3A). Longitudinal sections of wild-type limb buds revealed a distinct patch of *ALK7* mRNA expression, while no labeling could be observed in limb buds from *ALK7* mutant mice (Fig. 3B). Interestingly, mice carrying mutations in *ActRIIA* and *ActRIIB* have defects in axial vertebral patterning and limb skeletal malformations (14, 15). However, no skeletal abnormalities could be observed in mice lacking ALK7. The numbers of ribs and vertebrae were normal, and no limb or digit malformations, including webbing, could be detected in $ALK7^{-/-}$ mice (Fig. 3C and data not shown).

No left-right patterning defects in mice lacking ALK7. Given the prominent role of Nodal signaling in left-right patterning, we investigated possible alterations in the positioning of several organs in *ALK7* mutant mice. Fifty-nine $ALK7^{-/-}$ newborn mice (35 in inbred Sv129 and 24 in mixed Sv129 × C57BL/6 backgrounds, respectively) were examined for left-right patterning defects, including heart apex, gut looping, pulmonary isomerism, rostro-caudal position of the kidneys, and position of spleen and stomach. No left-right patterning defects were seen in any of the animals examined (Figs. 4A and B and data not shown). In ad-

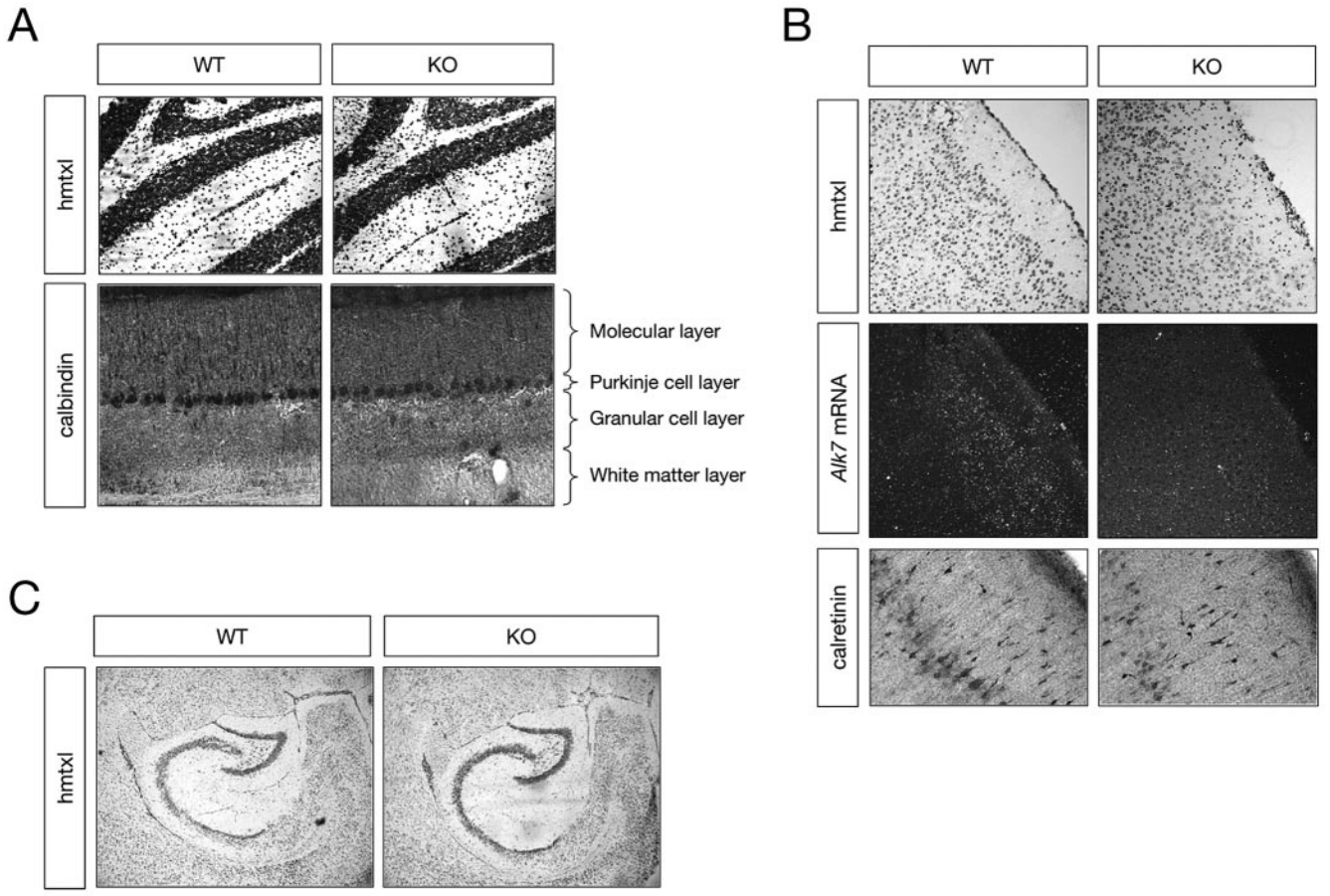

FIG. 5. No histological abnormalities in cerebella, cortices, and hippocampi of *ALK7* mutant mice. (A) Histological analysis of sections through the adult cerebellum of wild-type (WT) and *ALK7* mutant (knockout [KO]) mice. Hematoxylin (hmtxl) and Calbindin stainings are shown. Cerebellar layers are indicated. (B) Histological analysis of sections through the adult cerebral cortex of wild-type and *ALK7* mutant mice. Hematoxylin staining, *ALK7* mRNA in situ hybridization, and Calretinin immunohistochemistry are shown. (C) Histological analysis of sagittal sections through the adult hippocampus of wild-type and *ALK7* mutant mice. Hematoxylin staining is shown.

dition, no signs of spleen hypoplasia, a phenotype found in compound *ActRIIA ActRIIB* mutant mice (11), could be detected in *ALK7*$^{-/-}$ mice (Fig. 4C).

No histological abnormalities in cerebella, cortices, and hippocampi of *ALK7* mutant mice. Because of the predominant expression of *ALK7* in the postnatal central nervous system, particularly in cerebellum, cortex, and hippocampus (12, 17, 20), we also investigated possible histological abnormalities in the brains of adult *ALK7* mutant mice. Hematoxylin staining of cryostat sections of adult cerebellum revealed a normal lobation and lamination, with normal thicknesses of molecular and granule cell layers (Fig. 5A). Purkinje cells, which express high levels of *ALK7* mRNA (17), were found in normal numbers, and no defects could be observed in their arborization as assessed by Calbindin immunohistochemistry (Fig. 5A). Cortical lamination appeared normal in cryosections of *ALK7*$^{-/-}$ brains stained with hematoxylin (Fig. 5B). Moreover, no abnormalities in cell migration or positioning could be detected in postnatal day 6 cortex by using Calretinin immunohistochemistry (Fig. 5B), which predominantly labels inhibitory interneurons in the cortex. Finally, the histological organization of the hippocampus also appeared to be normal in *ALK7* mutant mice as assessed by hematoxylin staining (Fig. 5C).

DISCUSSION

The secreted factor Nodal has been shown to play a crucial role in at least four developmental processes: mesendoderm formation (5, 25), elongation of the primitive streak (13, 19), formation of the anterior head (19), and left-right patterning (13, 15, 23). Nodal has been shown to interact with two type I and two type II receptor serine/threonine kinases, namely, ALK4, ALK7, ActRIIA, and ActRIIB. ALK4 is known to contribute to mesendoderm formation in the mouse (9), but due to the early lethality of *ALK4* null mutants, the role of ALK4 in anterior head formation and left-right patterning remains to be demonstrated. On the other hand, all four Nodal-related phenotypes can be phenocopied in *ActRIIA ActRIIB* compound mutant mice (14, 15, 19). In addition, the Nodal EGF-CFC coreceptors Cripto and Cryptic have also been implicated in left-right patterning by genetic experiments (7, 23).

In this study, we report the generation and initial characterization of mutant mice lacking ALK7. None of the known Nodal-related phenotypes could be found in these mice, suggesting that ALK7 is not an obligatory component of the Nodal signaling pathway, at least during early development. It should be noted, however, that due to possible compensatory effects by *ALK4* and

other genes in this pathway, the participation of ALK7 in Nodal signaling cannot be completely ruled out at present. The gene network responsible for Nodal function includes several genes in addition to *Nodal* itself, such as those encoding type I and type II receptors; EGF-CFC coreceptors; Smad2, -3, and -4; and others. Previous genetic studies have indicated that this gene network is robust to different types of perturbations, suggesting that the true contribution of individual network components may emerge only through the generation and analysis of compound mutations. In an effort to address this problem, we have initiated the analysis of intercrosses between *ALK7* mutants and mouse lines carrying mutations in other components of this gene network. In the present study, we generated $ALK7^{-/-}$; $Nodal^{+/-}$ and $ALK7^{-/-}$; $ALK4^{+/-}$ compound mutants but found no reduction in viability at weaning compared to $ALK7^{-/-}$ or wild-type mice. However, as our analysis was necessarily limited to the use of heterozygous mutants for *Nodal* and *ALK4*, it is possible that both of these genes are expressed in sufficient excess during development to preclude haploinsufficiency effects in the absence of ALK7. Only after analysis of further crosses between *ALK7* mutants and other mouse lines, such as those carrying mutations in *Cripto*, *ActRIIA*, and *ActRIIB*, will it be possible to fully establish the role of ALK7 in Nodal signaling during mouse development.

The expression pattern of *ALK7* during postnatal and adult stages indicates possible functional roles in several tissues and organs. Because some of the most prominent sites of *ALK7* expression have been localized to the postnatal and adult central nervous system, we have investigated possible abnormalities in several brain regions where expression of this receptor is particularly concentrated, including cerebellum, cortex, and hippocampus. Our analyses, however, have not revealed major histological defects in any of those structures in *ALK7* mutant mice. More detailed anatomical and functional studies, including perhaps stress paradigms, will be required to elucidate the precise function of ALK7 in the mammalian brain. Because of the significant functional overlap with ALK4, future studies on the role of ALK7 in the brain may also require examination of compound mutant animals with conditional mutations in the *ALK4* locus. Finally, *ALK7* expression has also been detected in a few peripheral organs, including kidney, ovary, and pancreas (12, 17, 20). The mutant animals described in this study open the possibility to investigate possible functions of this receptor and the Nodal signaling pathway in several other tissues and organs.

ACKNOWLEDGMENTS

We thank Patrik Ernfors for advice regarding construction of targeting vectors, Elizabeth Robertson for *Nodal* mutant mice, En Li for *ALK4* mutant mice, Dagmar Galter for assistance with radioactive in situ hybridization, and Xiaoli Li for secretarial help.

This work was funded by grants from the Swedish Foundation for Strategic Research, the Swedish Cancer Society (3474-B97-05XBC), and the Swedish Medical Research Council (K99-33X-10908-06C). E.R. was supported during part of this project by an Individual Marie Curie Fellowship.

ADDENDUM IN PROOF

The role of ALK4 in left-right axis determination has been documented in a recent study (Y. Chen, E. Mironova, L. L. Whitaker, L. Edwards, H. J. Yost, and A. F. Ramsdell, Dev. Biol. **268:**280–294, 2004).

REFERENCES

1. **Armes, N. A., and J. C. Smith.** 1997. The ALK-2 and ALK-4 activin receptors transduce distinct mesoderm-inducing signals during early Xenopus development but do not co-operate to establish thresholds. Development **124:** 3797–3804.
2. **Brennan, J., D. P. Norris, and E. J. Robertson.** 2002. Nodal activity in the node governs left-right asymmetry. Genes Dev. **16:**2339–2344.
3. **Chang, C., P. A. Wilson, L. S. Mathews, and A. Hemmati-Brivanlou.** 1997. A Xenopus type I activin receptor mediates mesodermal but not neural specification during embryogenesis. Development **124:**827–837.
4. **Collignon, J., I. Varlet, and E. J. Robertson.** 1996. Relationship between asymmetric nodal expression and the direction of embryonic turning. Nature **381:**155–158.
5. **Conlon, F. L., K. M. Lyons, N. Takaesu, K. S. Barth, A. Kispert, B. Herrmann, and E. J. Robertson.** 1994. A primary requirement for nodal in the formation and maintenance of the primitive streak in the mouse. Development **120:**1919–1928.
6. **Ding, J., L. Yang, Y. T. Yan, A. Chen, N. Desai, A. Wynshaw-Boris, and M. M. Shen.** 1998. Cripto is required for correct orientation of the anterior-posterior axis in the mouse embryo. Nature **395:**702–707.
7. **Gaio, U., A. Schweickert, A. Fischer, A. N. Garratt, T. Muller, C. Ozcelik, W. Lankes, M. Strehle, S. Britsch, M. Blum, and C. Birchmeier.** 1999. A role of the cryptic gene in the correct establishment of the left-right axis. Curr Biol. **9:**1339–1342.
8. **Galter, D., A. Carmine, S. Buervenich, G. Duester, and L. Olson.** 2003. Distribution of class I, III and IV alcohol dehydrogenases mRNAs in the adult rat, mouse and human brain. Eur. J. Biochem **270:**1316–1326.
9. **Gu, Z., M. Nomura, B. B. Simpson, H. Lei, A. Feijen, J. van den Eijnden-van Raaij, P. K. Donahoe, and E. Li.** 1998. The type I activin receptor ActRIB is required for egg cylinder organization and gastrulation in the mouse. Genes Dev. **12:**844–857.
10. **Jörnvall, H., A. Blokzijl, P. ten Dijke, and C. F. Ibáñez.** 2001. The orphan receptor serine-threonine kinase ALK7 signals arrest of proliferation and morphological differentiation in a neuronal cell line. J. Biol. Chem. **276:**5140–5146.
11. **Kim, S. K., M. Hebrok, E. Li, S. P. Oh, H. Schrewe, E. B. Harmon, J. S. Lee, and D. A. Melton.** 2000. Activin receptor patterning of foregut organogenesis. Genes Dev. **14:**1866–1871.
12. **Lorentzon, M., B. Hoffer, T. Ebendal, L. Olson, and A. Tomac.** 1996. Habrec1, a novel serine/threonine kinase TGF-beta type I-like receptor, has a specific cellular expression suggesting function in the developing organism and adult brain. Exp. Neurol. **142:**351–360.
13. **Lowe, L. A., S. Yamada, and M. R. Kuehn.** 2001. Genetic dissection of nodal function in patterning the mouse embryo. Development **128:**1831–1843.
14. **Oh, S. P., and E. Li.** 1997. The signaling pathway mediated by the type IIb activin receptor controls axial patterning and lateral asymmetry in the mouse. Genes Dev. **11:**1812–1826.
15. **Oh, S. P., C. Y. Yeo, Y. Lee, H. Schrewe, M. Whitman, and E. Li.** 2002. Activin type IIA and IIB receptors mediate Gdf11 signaling in axial vertebral patterning. Genes Dev. **16:**2749–2754.
16. **Reissmann, E., H. Jörnvall, A. Blokzijl, O. Andersson, C. Chang, G. Minchiotti, M. Persico, C. F. Ibáñez, and A. H. Brivanlou.** 2001. The orphan receptor ALK7 and the Activin receptor ALK4 mediate signaling by Nodal proteins during vertebrate development. Genes Dev. **15:**2010–2022.
17. **Rydén, M., T. Imamura, H. Jörnvall, N. Belluardo, I. Neveu, M. Trupp, T. Okadome, P. ten Dijke, and C. F. Ibáñez.** 1996. A novel type I serine-threonine kinase receptor predominantly expressed in the adult central nervous system. J. Biol. Chem. **271:**30603–30609.
18. **Schier, A. F.** 2003. Nodal signaling in vertebrate development. Annu. Rev. Cell Dev. Biol. **19:**589–621.
19. **Song, J., S. P. Oh, H. Schrewe, M. Nomura, H. Lei, M. Okano, T. Gridley, and E. Li.** 1999. The type II activin receptors are essential for egg cylinder growth, gastrulation, and rostral head development in mice. Dev. Biol. **213:**157–169.
20. **Tsuchida, K., P. E. Sawchenko, S. I. Nishikawa, and W. W. Vale.** 1996. Molecular cloning of a novel type I receptor serine/threonine kinase for the TGF-beta superfamily from rat brain. Mol. Cell Neurosci. **7:**467–478.
21. **Watanabe, R., Y. Yamada, Y. Ihara, Y. Someya, A. Kubota, S. Kagimoto, A. Kuroe, T. Iwakura, Z. P. Shen, A. Inada, T. Adachi, N. Ban, K. Miyawaki, Y. Sunaga, K. Tsuda, and Y. Seino.** 1999. The MH1 domains of Smad2 and Smad3 are involved in the regulation of the ALK7 signals. Biochem. Biophys. Res. Commun. **254:**707–712.
22. **Wilkinson, D. G.** 1992. In situ hybridization: a practical approach. Oxford University Press, London, United Kingdom.
23. **Yan, Y. T., K. Gritsman, J. Ding, R. D. Burdine, J. D. Corrales, S. M. Price, W. S. Talbot, A. F. Schier, M. M. Shen, L. A. Lowe, S. Yamada, and M. R. Kuehn.** 1999. Conserved requirement for EGF-CFC genes in vertebrate left-right axis formation. Genes Dev. **13:**2527–2537.
24. **Yeo, C. Y., and M. Whitman.** 2001. Nodal signals to Smads through Cripto-dependent and Cripto-independent mechanisms. Mol. Cell **7:**949–957.
25. **Zhou, X., H. Sasaki, L. Lowe, B. L. Hogan, and M. R. Kuehn.** 1993. Nodal is a novel TGF-beta-like gene expressed in the mouse node during gastrulation. Nature **361:**543–547.